An Electrochemical Sensor Based on Multi-Walled Carbon Nanotubes Functionalized with 2-Picolinyl Hydrazide for Electrochemical Detection of Pb(II) Ions

Li, Zhenliang*+; Liu, Xuerui; Li, Shuye

College of Chemistry and Chemical Engineering, Ningxia Normal University, Guyuan, Ningxia 756000, P.R. CHINA

ABSTRACT: *A new electrochemical sensor was constructed with the nanometer coaxial cable, which was prepared based on Multi-Walled Carbon NanoTubes (MWCNTs) and pyridine. the analysis of trace Pb(II) with Differential Pulse Anodic Stripping Voltammetry (DPASV) was studied. The MWCNTs–TPI–2–Ph was characterized by SEM, TEM, and electrochemical methods. Various parameters such as deposition time, pH values, deposition potential, interference experiment, stability, and reproducibility were investigated. DPASV was used for evaluating the detection of trace Pb(II) based on the accumulation process. Under the optimal conditions, the MWCNTs–TPI–2–Ph/GCE showed excellent stripping response of Pb(II) in the ranges of 1 to 100 μmol/L, the peak currents linearly increased with the concentration of Pb(II). The detection limit was calculated to be 0.03 μM (S/N=3). Detection mechanism for Pb(II) based on MWCNTs–TPI–2–Ph/GCE was proposed. Therefore, it was essential to design an electrochemical sensor based on a new metal ions capture reagent.*

KEYWORDS: *Nanometer coaxial cable; pulse anodic stripping voltammetry; Multi-walled carbon nanotubes; Heavy metal ions; Electrochemical sensor.*

INTRODUCTION

Heavy Metal Ions (HMI) are terrible contributors to water pollution because of their highly toxic, non-degradable character, once in the food chain, bioaccumulation and biomagnification would appear, which will affect the living systems as time goes on both in aquatic ecosystems and the soil environment, HMI is very dangerous to the whole community of ecology of plants, humans, and animals [1]. In recent years, more and more researchers have paid more attention to the measurements of HMI in environment protection, food firms, and biomedical analysis [2]. Nowadays, HMI detection techniques were developed quickly, which included inductively coupled plasma mass spectroscopy, atomic absorption spectrometry, atomic fluorescence spectrometry, X-Ray fluorescence spectrometry, and electrochemical methods of detection [3-4], etc. However, which can offer highly sensitive and selective detection methods of HMI, high cost and long detection time limited its wider application. A large number of researchers were attracted to the field of HMI electrochemical detection with low cost, high sensitivity, and time economics.

* *To whom correspondence should be addressed.*
+ E-mail: guliang110@sohu.com
1021-9986/2022/5/1528-1537 10/$/6.00

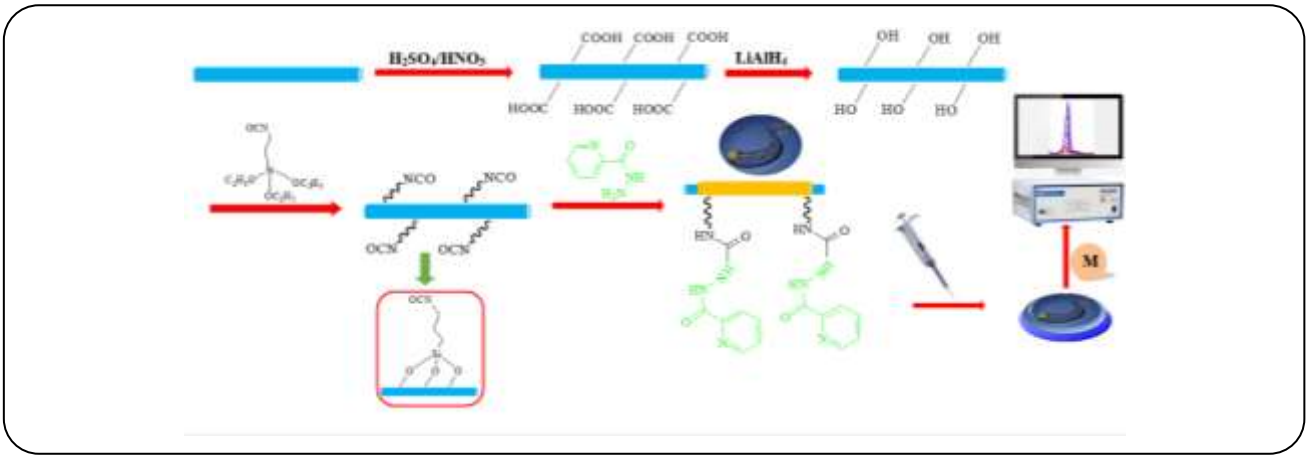

Fig. 1: Schematic of the MWCNTs–TPI–2–Ph/GCE construction and the determination process of Pb(II).

Therefore, chemically-modified electrodes have been introduced to HMI detection based on carbon-based materials [5], noble metallic nanoparticles, and silicon-based materials [6, 7], Furthermore, small organic molecular, polymer, and inorganic-organic nanocomposite anchoring to the materials, nanocomposite modified electrodes have significantly improved sensitivity and selectivity of sensors [8-9]. Ramírez María has developed an electrochemical biosensor for Pb(II) based on single-walled carbon nanotubes covalently modified with cysteine [10]. Zhao reported an electrochemical sensor for the simultaneous determination of Pb(II) and Cd(II) based on L-cysteine functionalized single-walled carbon nanotubes incorporating nafion and ionic liquid [11]. *Deshmuk* prepared an electrochemical platform for the determination of copper(II), lead(II), and mercury(II) ions based on ethylenediaminetetraacetic acid-modified single-walled carbon nanotubes [12]. *Bagheri* research group has developed a series of innovative platforms for HMI based on Multi-Walled Carbon NanoTubes (MWCNTs) [13,14], graphene [15], and SiO_2 nanoparticles [16].

Inspired by pyridine which can form complexes with some metal ions due to the unshared pair on the nitrogen, it is the perfect site to coordinate with metal ions based on 2-Picolinyl hydrazide [17-18]. Herein, we reported an efficient strategy of nanometer coaxial cable based on MWCNTs for electrochemical detection of Pb(II) ions. As shown in Fig. 1. It is a facile way that 2–Picolinyl hydrazide(Ph) was immobilized on MWCNT *via* 3–(Triethoxysilyl)propyl isocyanate (TPI). Then, MWCNTs–2–Ph was used to construct an electrochemical sensor for the detection of Pb(II) with DPASV and the results were satisfactory.

EXPERIMENTAL SECTION

Reagents and materials

The multi-walled carbon nanotubes (MWCNTs) were purchased from Shenzhen Bier Technology Co., Ltd (Shenzhen, China). 3–(Triethoxysilyl)propyl isocyanate (TPI) and 2–Picolinyl hydrazide (2–Ph) were purchased from Aladdin Industrial Corporation. Stock solutions of Pb(II) were obtained from lead nitrate, HAc–NaAc buffer solutions were prepared by mixing stock solutions of 1 M/L NaAc and 1 M/L HAc. All other reagents of analytical grade were commercially available without further purification. Ultrapure water was used throughout the experiments.

Apparatus

The materials were synthesized and characterized by Fourier–transform infrared Spectra spectrometer (Thermo Fisher Scientific Nicolet iS5 FTIR), X-ray photoelectron spectroscopy (Thermo Fisher ESCALAB 250Xi, XPS), Scanning electron microscopy (Carl Zeiss Gemini 300, SEM) Transmission electron microscope (JEOL JEM 2100F, TEM). All electrochemical tests were performed on a CHI660E electrochemical workstation (Shanghai Chenhua Instruments Co., China) with a conventional three-electrode system: a bare Glassy Carbon Electrode (GCE) or modified GCE served as the working electrode, a platinum wire as the counter-electrode, and a saturated calomel electrode.

Analytical experiments

The analysis of Pb(II) based on MWCNTs–TPI–2–Ph involved two steps: an electrochemical accumulation step

at open circuit and an anodic stripping voltammetric step. For the accumulation step, the MWCNTs–TPI–2–Ph/GCE was immersed into 10 mL of supporting electrolyte (1mol/L HAc–NaAc, pH=5.0) containing the Pb(II), to allow pre-concentration of the target analyte at a constant potential (–1.2 V) for 300 s. After 20 seconds, in the anodic stripping process. Then the anodic stripping peak current was obtained by the Differential Pulse Voltammetric (DPV) measurement from –1.0 V to –0.3 V. The DPV parameters are as follows: –1.2 V deposition potential, 50 Hz frequency, 0.05 V potential amplitude. Prior to the next cycle, the modified electrode was cleaned by applying a potential of 120 s at +1.2 V under stirring.

Preparation of MWCNTs-OH

The MWCNTs–COOH was synthesized as previously reported methods [19-20]. In the second step, the MWCNTs–COOH reacted with $LiAlH_4$ in dry tetrahydrofuran at room temperature for 12 h, which products were hydroxyl group functionalized MWCNTs (MWCNTs–OH).

Preparation of MWCNTs-2-Ph nanocomposites

TPI-functionalized MWCNTs were synthesized according to previous literature [21-22]. 0.31 g TPI was dissolved into 50 mL of dry toluene solution in a round-bottom flask. Next, 1 g of MWCNTs–OH was dispersed in the above solution *via* ultrasonication 10 min. Then the mixture was refluxed at 110 ℃ 12 h under stirring. Afterward, the products were washed with toluene many times, the MWCNTs–TPI were obtained and dispersed in 100 mL acetonitrile *via* ultrasonication 10 min [23]. 2-Ph was added to the above acetonitrile solution stirring at 82℃ for 12 h, and finally, the products were washed with ethanol and dichloromethane, respectively. MWCNTs-TPI-2-Ph was obtained and vacuum dried at 50 ℃ for 5 h.

Preparation of modified electrode

The MWCNTs-TPI-2-Ph nanocomposites were dispersed into ultrapure water *via* ultrasonic agitation for 30 min. Prior to the Glass Carbon Electrode (GCE) modification, the GCE was polished carefully with 1.0, 0.3, and 0.05 μm of alumina powder, respectively, rinsed and sonicated with alcohol and ultrapure water successively, and dried under nitrogen. Then, 6 μL of the sonicated solution was pipetted onto the surface of GCE with 3.0 mm in diameter, and then, the solvent was evaporated under UV lamp to obtain the MWCNTs-TPI-2-Ph nanocomposite film-modified GCE [24].

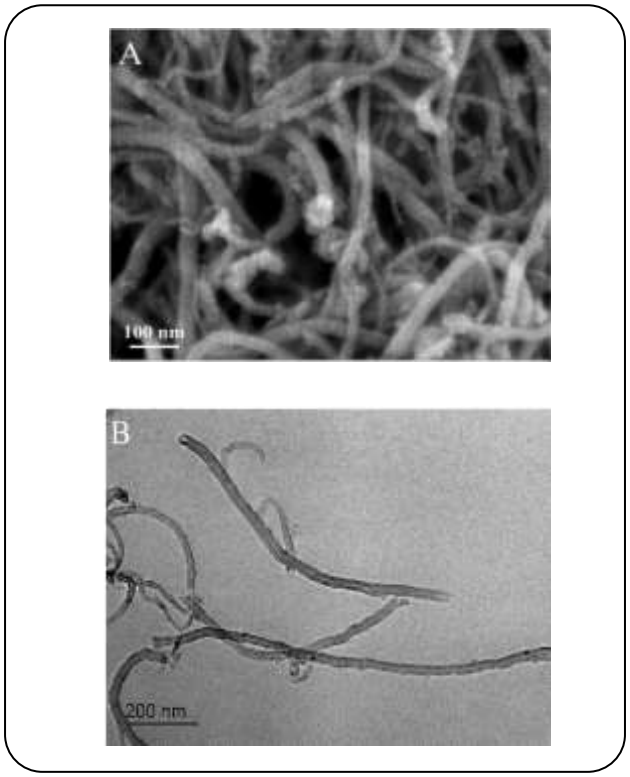

Fig. 2: SEM (A) and TEM images(B) of MWCNTs–TPI–2–Ph.

RESULTS AND DISCUSSION

Characterization of MWCNTs–TPI–2–Ph composites

The surface morphologies of the nanometer coaxial cable based on MWCNTs were investigated with SEM and TEM. Obviously, the nanotubes in Fig. 2(A) appeared with a rough surface, which indicated that MWCNTs were coated with silica-organic ligand film to form a cable-like structure [25]. It is noted that 2–Ph was immobilized on the MWCNTs with TPI. Fig. 2 B shown two typical TEM images of MWCNTs-TPI-2-Ph were prepared successfully and remained uniform thickness during the entire process of silica-organic ligand coating, which implied that TPI was linked to the MWCNTs. Moreover, the nanometer coaxial cable structure was confirmed by TEM images [26].

The FT-IR spectra of MWCNTs–COOH(a), MWCNTs–OH(b), and MWCNTs–TPI–2–Ph(c) were shown in Fig. S1. The characteristic peaks of MWCNTs–COOH appeared in curve a, the stretching vibration band of O–H appeared at 3436 cm^{-1}, The peak at 1707 cm^{-1} may attribute to

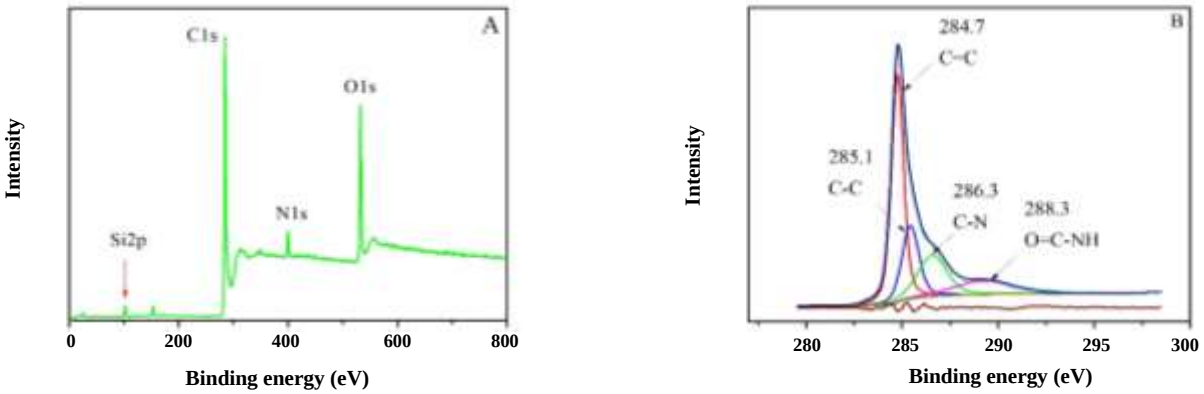

Fig. 3: XPS spectrum of the MWCNTs–TPI–2–Ph synthesized.

C=O stretching of carboxyl groups and the peaks in 1460–1640 cm^{-1} range are ascribed to the stretching vibration of backbone C=C of MWCNTs–COOH [27]. In curve b, the vibrational band was located at 1630 cm^{-1}, which is ascribed to a stretching mode of OH group in an enol C=C–OH. The peaks were broadened at 2934 cm^{-1} and 3436 cm^{-1} due to the hydroxyl associating, which indicated that carboxyl groups were reduced with lithium aluminum hydride at large [28]. In curve c, the –Si–O–Si– band appeared at 780 and 1081 cm^{-1}, and the characteristic peaks at around 3000-2800 cm^{-1} were assigned to aliphatic C–H stretching vibrations. Moreover, the peaks at 1576cm^{-1}, 1477cm^{-1}, 1340 cm^{-1} were attributed to C=N, C–N, and C–H bending vibrations of the linked isocyanate, respectively [29]. The evidence suggested that the 2–Ph had been linked to MWCNTs–OH with TPI.

The chemical bonding of synthesized MWCNTs–TPI–2–Ph was investigated by XPS. C, N, and a small amount of O constitute MWCNTs–TPI–2–Ph as shown in Fig. 3 (A) [30]. The XPS spectrum of C1s was presented in Fig. 3 (B), the sharp characteristic peaks centered at 284.7 eV, 285.1 eV, and 286.3 eV, which were exclusively attributed to C=C, C–C, and C–N, respectively. The peak at 288.3 eV corresponds to O=C–NH, which indicated that the conversion of O=C–NH was successful [31]. As expected, 2-Ph was linked to TPI. Moreover, according to the FT-IR spectra, SEM, and TEM image, 2–Ph was coated on the MWCNTs by TPI as the crosslinking agent.

Optimization of experimental conditions

In order to obtain sensitivity for Pb(II) detection with MWCNTs–TPI–2–Ph modified GCE, the voltammetric parameters were optimized in a solution containing 100 μM Pb(II), such as pH value, deposition potential, and deposition time. The pH value of the buffer solution has an effect on the DPASV response, it is essential to look for the optimal pH value, the influence of buffer solution with different pH values was investigated in Fig. S2, the pH ranged from 3.0 to 6.5 in 1 M/L acetate buffer solution [32]. In Fig. S2(A), the stripping peak current of Pb(II) increased with increasing pH values in 0.1 M acetate buffer solution until 5.0, the maximum current response appeared at pH 5.0. Therefore, pH=5.0 was selected as the optimal pH in this work. Thus, the effect of the deposition potential was studied after 300 s accumulation in the range from −1.0 to −1.7 V at pH 5.0. The obtained results were shown in Fig. S2(B). When the deposition potential increased from −1.0 to −1.2 V, and the maximum of peak currents was obtained at potential −1.2 V. When a deposition potential was shifted to −1.7 V, the stripping currents decreased observed for Pb(II). Obviously, −1.2 V was the optimal deposition potential in the subsequent work. Adequate deposition time plays a very important role in stripping analysis. The effect of deposition time was estimated in the range 120−420 s for a solution containing 100 μM/L Pb(II), the dependence of peak currents on the deposition time was depicted in Fig. S2(C), which implied that increasing deposition time was a benefit for the detection of very low concentration of Pb(II). However, 300 s was optimized deposition in this experiment.

Electrochemical properties of different modified electrodes

The cyclic voltammetric response of bare GCE, MWCNTs/GCE, and MWCNTs–TPI–2–Ph/GCE have been investigated in 5 mM $Fe(CN)_6^{3-/4-}$ in Fig. 4A.

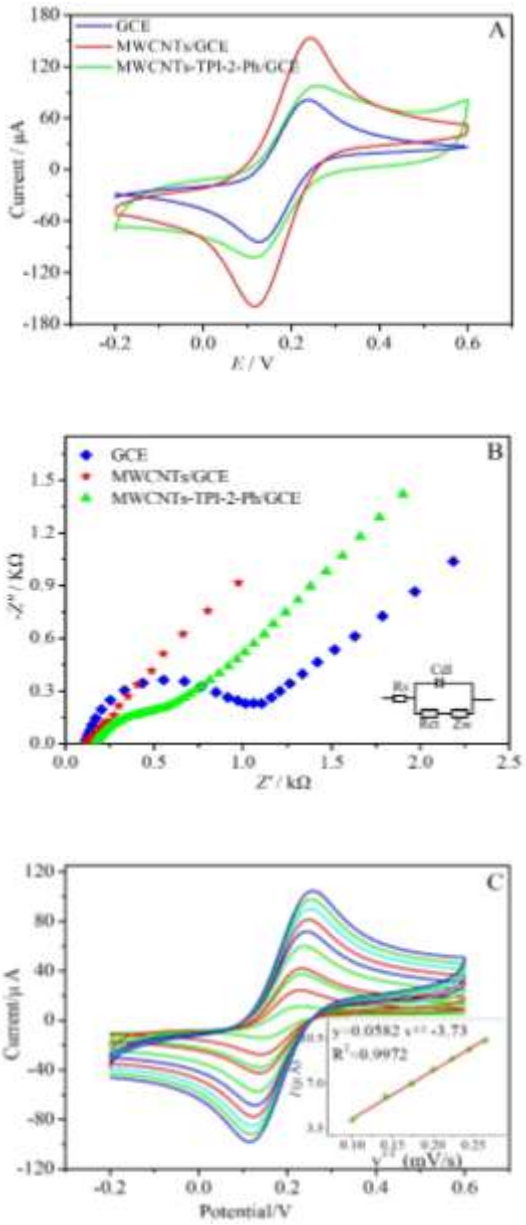

Fig. 4: Cyclic voltammetric response recorded with bare GCE, MWCNTs/GCE, and MWCNTs–TPI–2–Ph/GCE in the solution of 5 mM $Fe(CN)_6^{3-/4-}$(A), Nyquist plots at GCE, MWCNTs/GCE and MWCNTs–TPI–2–Ph/GCE in 5 mM $Fe(CN)_6^{3-/4-}$(B). The cyclic voltammetric response of MWCNTs–TPI–2–Ph/GCE at various scan rates ranging from 0.001-0.070 Vs^{-1}. Inset: Plot of stripping peak current vs square root of scan rate (C).

There are well-defined redox peaks based on bare GCE, as compared with the bare GCE, the peak currents increased at MWCNTs modified electrode, which indicated that the rate of electron transfer was accelerated due to good conductivity. After modification with the MWCNTs–TPI–2–Ph nanocomposites, the lowest current was obtained at the modified electrode, which revealed that the rate of electron transfer was hindered due to the silica-organic ligand film coated on the MWCNTs. The further interface properties of modified electrodes were provided by the electrochemical impedance spectrum (EIS). In a typical Nyquist plot, as seen in Fig. 4B, the electron transfer resistance (R_{et}) values of bare GCE and MWCNTs/GCE were about 1096 Ω, 317 Ω, respectively. After modification with MWCNTs–TPI–2–Ph, The R_{et} of MWCNTs–TPI–2–Ph/GCE was 759 Ω, which was ascribed to the poor conductivity of silica-organic ligand film at the modified electrode surface [33]. The R_{et} value was consistent with the cyclic voltammetric response. The cyclic voltammetric response of MWCNTs–TPI–2–Ph/GCE at different scan rates was shown in Fig. 4(C), the equivalent circuits were provided based on the interfacial electron transfer resistance of modified electrodes. Moreover, the inset of Fig. 4(C) showed the plot of stripping peak current vs square root of scan rate, which indicated the process was controlled by diffusion.

Stripping behavior toward Pb(II)

The DPV curves with different concentrations of Pb(II) were investigated with the MWCNTs–TPI–2–Ph modified electrode under the optimized conditions in Fig. 5A, and the corresponding standard curve was presented. Obviously, the stripping peak currents increased with the increasing concentration of Pb(II). As shown in Fig. 5B, the linear equation was I / μA= 9.81 + 1.81c / μM, (R^2=0.9921, LOD=0.03 μM) The Limit of Detection (LOD) was obtained with the result of 0.03 μM.

Evaluation of stability and reproducibility

The stability of the MWCNTs–TPI–2–Ph/GCE was investigated based on the same electrode, which was repeatedly performed eight times at the optimum condition. As shown in Fig. 6, the stripping currents of MWCNTs–TPI–2–Ph/GCE were recorded with a relative standard deviation (RSD) of 3.67 %, it is indicated that modified electrodes were stable, the nanocomposite of MWCNTs–TPI–2–Ph on the surface had not detached. which implied that the stability of the modified electrode was accepted. Meanwhile, MWCNTs–TPI–2–Ph/GCE was prepared based on four GCE at the same procedure, which was used to detect 60 μM/L Pb(II) under the optimized

Table 1: The different electrochemical sensors for the determination of Pb(II).

Modified electrode	Electrochemical methods	ions	Linear range	Detection limit	Ref.
Sb_2O_3/MWCNTs/GCE	LASV	Pb(II)	5–35 µg/L	5–35 µg/L	[36]
PGA/rGO/GCE	SWASV	Pb(II)	0.2–115 µg/L	0.06 µg/L	[37]
Bi/Au-GN-Cys/GCE	SWASV	Pb(II)	0.5–40 µg/L	0.05 µg/L	[38]
N,S–YS–900/Nafion/Bi/GCE	DPASV	Pb(II)	4–160 µg/L	0.49 µg/L	[39]
MWCNTs/Nafion/Bi/GCE	DPASV	Pb(II)	0.5–30 µg/L	0.02 µg/L	[40]
Fe_3O_4@G2–PAD	SWASV	Pb(II)	0.5–80 µg/L	0.17 µg/L	[41]
SWCNs/L-Cys/Nafion-IL/GCE	SWASV	Pb(II)	0–50 µg/L	0.08 µg/L	[42]
MWCNTs–TPI–2–Ph/GCE	DPASV	Pb(II)	1–100 µM/L	0.03 µM/L	This work

Linear anodic stripping voltammetry (LASV); Square wave voltammetry (SWAV); differential pulse anodic stripping voltammetry (DPASV).

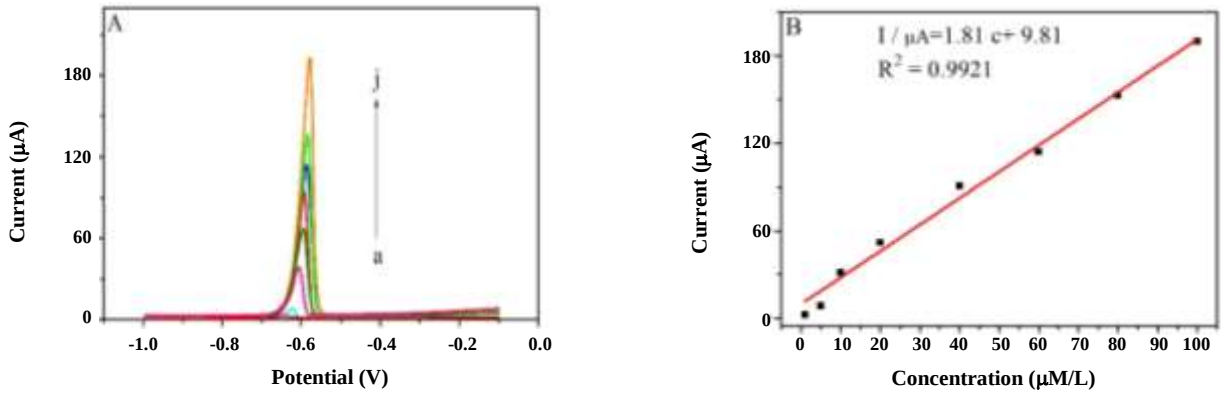

Fig. 5: (A) DPV responses at MWCNTs–TPI–2–Ph modified electrode with different concentrations, from a to j: 1, 5, 10, 20, 30, 40, 50, 60, 80 and 100 µM/L. Deposition potential= −1.2 V; pH=5.0; deposition time=300 s. (B)The calibration plot of peaks current versus the Pb(II) concentration.

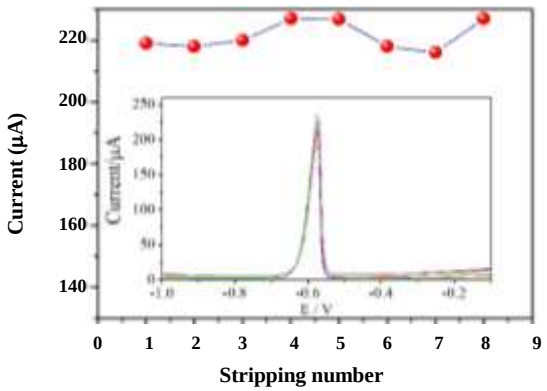

Fig. 6: ***The stability of MWCNTs–TPI–2–Ph/GCE (eight times) of DPASV responses for 100 µM/L Pb(II) in 1 M/L NaAc-HAc buffer solution at the optimum conditions: pH=5.0, deposition potential= −1.2 V, deposition time=300 s. Inset: DPV responses for 100 µM/L Pb(II) on the MWCNTs–TPI–2–Ph/GCE under eight times scans.***

condition to estimate the reproducibility. The RSD of stripping peak currents obtained was 5.02 %, which indicated the reproducibility was acceptable.

Detection mechanism

The detection mechanism was demonstrated in Fig.7, Pb(II) can be directly reduced and oxidized on the surface of MWCNTs. With the synergistic catalysis effect of MWCNTs, metal ions capture reagent greatly enhances the sensitivity to Pb(II), and the active sites play an important role in the detention of Pb(II).

Interference measurements

The interference of some foreign ions was investigated under the optimal conditions, which included SO_4^{2+}, NO_3,

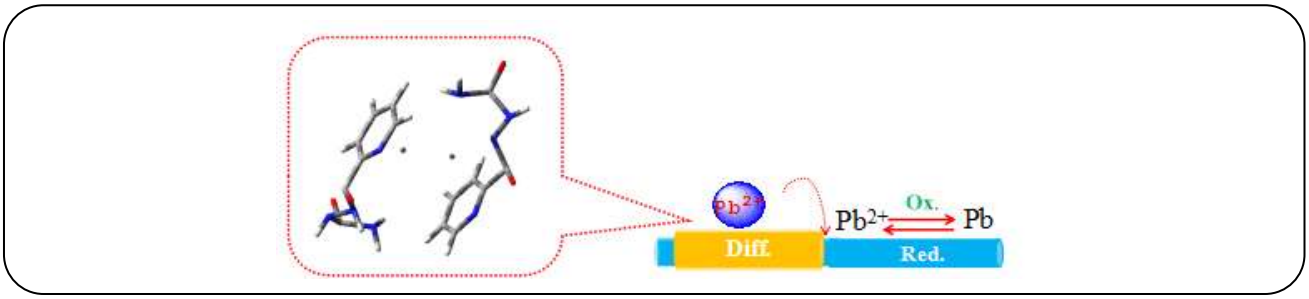

Fig. 7: Synergistic catalysis mechanism proposed toward Pb(II) based on MWCNTs–TPI–2–Ph.

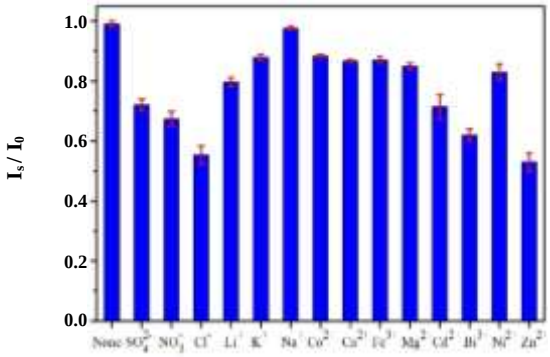

Fig. 8: The interference experiment result of MWCNTs–TPI–2–Ph/GCE at Pb(II) in the presence of possible interference ions.

Cl^-, Li^+, Co^{2+}, K^+, Fe^{3+}, Ca^{2+}, Mg^{2+}, Na^+, Cd^{2+}, Bi^{3+}, Ni^{2+} and Zn^{2+}. The selectivity of the MWCNTs–TPI–2–Ph/GCE was estimated by peak current ratio (I_s/I_0), the stripping peak responses of Pb(II) were recorded in the presence (I_s) and absence of interfering ions (I_0), respectively. As shown in Fig. 8, 5-fold excess of Na^+ did not affect the electrochemical response. The interference of SO_4^{2+}, NO_3^-, and Cl^- should not be ignored, therefore, it is important to improve the selectivity of MWCNTs–TPI–2–Ph/GCE for heavy metal ions.

CONCLUSIONS

The nanometer coaxial cable based on MWCNTs was prepared, 2-Ph was the perfect metal ion capture reagent with pyridine and hydrazine group, which was immobilized on the MWCNTs effectively by covalent bonding. MWCNTs–TPI–2–Ph modified electrode was used for the detection of ultra-trace Pb(II) ions, and the results were satisfactory. Therefore, amino groups and hydrazine groups play an important role in the detection of ultra-trace Pb(II), and the design of a new metal ion capture reagent might give a direction for HMI detection.

Acknowledgments

This work was supported by the Research Plan Projects of Ningxia Normal University (NXSFZDA2004).

Received :May 11, 2021 ; Accepted : Jul. 5, 2021

REFERENCES

[1] Eshghi A., Kheirmand M., Surface modification of Glassy Carbon Electrode by Ni-Cu Nanoparticles as a Competitive Electrode For Ethanol Electro-Oxidation, *Iran. J. Chem. Chem. Eng. (IJCCE)*, **37(5)**: 1-8 (2018).

[2] Beitollahi H., Moghaddam H.M., Tajik S., Voltammetric Determination Of Bisphenol a in Water and Juice Using a Lanthanum (III)-Doped Cobalt (II, III) Nanocube Modified Carbon Screen-Printed Electrode, *Anal. Lett.*, **52(9)**:1432-1444 (2018).

[3] Afkhami A., Shirzadmehr A., Madrakian T. and Bagheri H., Improvement in the Performance of a Pb^{2+} Selective Potentiometric Sensor Using Modified Core/Shell SiO_2/Fe_3O_4 Nano-Structure, *J. Mol. Liq.*, **199**: 108-114 (2014).

[4] Ahmadian-Alam L., Teymoori M. and Mahdavi H., Graphene Oxide-Anchored Reactive Sulfonated Copolymer Via Simple one Pot Condensation Polymerization: Proton-Conducting Solid Electrolytes, *J. Polym. Res.*, **25(1)**:1-13 (2018).

[5] Kazemipour M., Ansari M., Mohammadi A., Be itollahi H., Ahmadi R., Use of Adsorptive Square-Wave Anodic Stripping Voltammetry at Carbon Paste Electrode for the Determination of Amlodipine Besylate in Pharmaceutical Preparations, *J. Anal. Chem.*, **64(1)**:65-70 (2009).

[6] Bansod B.K., Kumar T., Thakur R., Rana S., Singh I., A Review on Various Electrochemical Techniques for Heavy Metal Ions Detection with Different Sensing Platforms, *Biosens. Bioelectron*., **94**: 443-455 (2017).

[7] Bagheri H., Afkhami A., Khoshsafar H., Rezaei M., Sabounchei S.J., Sarlakifar M., Simultaneous Electrochemical Sensing of Thallium, Lead and Mercury Using a Novel Ionic Liquid/Graphene Modified Electrode, *Anal. Chim. Acta*., **870**: 56-66 (2015).

[8] Deshmuk M.A., Celiesiute R., Ramanaviciene A., Shirsat M.D., Ramanavicius A., EDTA PANI/SWCNTs Nanocomposite Modified Electrode for Electrochemical Determination of Copper (II), Lead (II) and Mercury (II) Ions, *Electrochim. Acta*., **259**: 930-938 (2018).

[9] Ganjali M.R., Dourandish Z., Beitollahi H., Tajik S., Hajiaghababaei L., Larijani B., Highly Sensitive Determination of Theophylline Based on Graphene Quantum Dots Modified Electrode, *Int. J. of Electrochem. Sc*., **13**: 2448-2461 (2018).

[10] Feminus J.J., Deepa P.N., Electrochemical Sensor Based on Composite of Reduced Graphene and Poly-Glutamic Acid for Selective and Sensitive Detection of Lead, *J Mater Sci-Mater El.*, **30(16)**: 15553-15562 (2019).

[11] Madadrang C.J., Kim H.Y., Gao G., Wang N., Zhu J., Feng H., Gorring M., Kasner M.L., Hou S.F., Adsorption Behavior of EDTA-Graphene Oxide for Pb (II) Removal, *ACS. Appl. Mater. Inter*., **4(3)**: 1186-1193 (2012).

[12] Hai T.L., Hung L.C., Phuong T.T., Ha B.T., Nguyen B.S., Hai T. D., Nguyen V. H., Multiwall Carbon Nanotube Modified by Antimony Oxide (Sb_2O_3/MWCNTs) Paste Electrode for the Simultaneous Electrochemical Detection of Cadmium and Lead Ions, *Microchemical Journal*., **153**: 104456-104480 (2020).

[13] Huang X.J., Zhou W.Y., Xiao X.Y., Chen S.H., Li S.S., Wang J., Synergistic Catalysis of N Vacancies and 5 nm Au Nanoparticles Promoted the Highly Sensitive Electrochemical Determination of Lead(II) Using an Au/N-Deficient-C_3N_4 Nanocomposite, *Environ. Sci. Nano*., **6(6)**: 1895-1908 (2019).

[14] Ji X., Chen Y., Wang X. Liu W., Sulphate-Functionalized Multi-Walled Carbon Nanotubes as Catalysts for the Esterification of Glycerol with Acetic Acid, *Kinet. Catal*., **52(4)**: 555-558 (2011).

[15] Tajik S., Dourandish Z., Zhang K., Beitollahi H., Le Q.V., Jang H.W., Shokouhimehr M., Carbon and Graphene Quantum Dots: A Review on Syntheses, Characterization, Biological and Sensing Applications for Neurotransmitter Determination, *RSC Adv.*, **10(26)**: 15406-15429 (2020).

[16] Li X., Zhou H., Fu C., Wang F., Ding Y., Kuang Y., A Novel Design of Engineered Multi-Walled Carbon Nanotubes Material and its Improved Performance in Simultaneous Detection of Cd(II) and Pb(II) by Square Wave Anodic Stripping Voltammetry, *Sensors and Actuat B-Chem*., **236**: 144-152 (2016).

[17] Liu Z., Liu Y. and Peng D., Hydroxylation of Multi-Walled Carbon Nanotubes Reduces their Cytotoxicity by Limiting the Activation of Mitochondrial Mediated Apoptotic Pathway, *J. Mater. Sci-Mater. M*., **25(4)**: 1033-1044 (2014).

[18] Lu Z., Yang S., Yang Q., Luo S., Liu C., Tang Y., A Glassy Carbon Electrode Modified with Graphene, Gold Nanoparticles and Chitosan for Ultrasensitive Determination of Lead(II), *Mikrochim Acta*, **180(7)**: 555-562 (2013).

[19] Moghaddam H. M., Beitollahi H., Tajik S., Jahani S., Khabazzadeh H., Alizadeh R., Voltammetric Determination of Droxidopa in the Presence of Carbidopa Using a Nanostructured Base Electrochemical Sensor, *Russ. J. Electrochem*., **53(5)**: 452-460 (2017).

[20] Mathew A., Parambadath S., Kim S.Y., Park S.S., Ha C.S., Adsorption of Cr(III) Ions Using 2-(ureylenemethyl)pyridine Functionalized MCM-41, *J. Porous Mat*., **22(3)**: 831-842 (2015).

[21] Beitollahi H., Khalilzadeh M. A., Tajik S., Safaei M. Shokouhimehr M., Recent Advances in Applications of Voltammetric Sensors Modified with Ferrocene and its Derivatives, *ACS Omega*, **5(5)**: 2049-2059 (2020).

[22] Mei J., Ying Z., Sheng W., Chen J., Zheng P., A Sensitive and Selective Electrochemical Sensor for the Simultaneous Determination of Trace Cd^{2+} and Pb^{2+}, *Chem. Pap*., **74(3)**: 1027-1037 (2019).

[23] Motaghi M., Beitollahi M.H., Tajik S., Hosseinzadeh R., Nanostructure Electrochemical Sensor for Voltammetric Determination of Vitamin C in the Presence of Vitamin B6: Application to Real Sample Analysis, *Int. J. of Electrochem. Sc*.,**11**: 7849-7860 (2016).

[24] Moghaddam H.M., Tajik Sand Beitollahi H., A New Electrochemical DNA Biosensor Based on Modified Carbon Paste Electrode Using Graphene Quantum Dots and Ionic Liquid for Determination of Topotecan – Sciencedirect, *Microchem. J*., **150**: 104085-104085 (2019).

[25] Priya T., Dhanalakshmi N., Thennarasu S., Karthikeyan V., Thinakaran N., Ultra Sensitive Electrochemical Detection of Cd^{2+} and Pb^{2+} Using Penetrable Nature of Graphene/Gold Nanoparticles/Modified L-Cysteine Nanocomposite, *Chem. Phys. Lett*., **731**: 136621-136628 (2019).

[26] Ramírez María L., Tettamanti C. S., Gutierrez F. A., Gonzalez-Domínguez J. M., Alejandro A. C., Javier H.F., Cysteine Functionalized Bio-Nanomaterial for the Affinity Sensing of Pb(II) as an Indicator of Environmental Damage, *Microchemical Journal*., **141**: 271-278 (2018).

[27] Sajid M., Bentonite-Modified Electrochemical Sensors: A Brief Overview of Features and Applications, *Ionics*., **24(1)**: 19-32 (2018).

[28] Tenorioalfonso A., Sanchez M. C. and Franco J. M., A Review of the Sustainable Approaches in the Production of Bio-Based Polyurethanes and Their Applications in the Adhesive Field, *J. Polym. Environ*., **28(3)**: 749-774 (2020).

[29] Wang S., Li J., Qiu Y., Zhuang X., Wu X., Jiang J., Facile Synthesis of Oxidized Multi-Walled Carbon Nanotubes Functionalized with 5-Sulfosalicylic Acid/MoS_2 Nanosheets Nanocomposites for Electrochemical Detection of Copper ions, *Appl. Surf. Sci*., **487**: 766-772 (2019).

[30] Wang H.Q., Xu R.Y., Chen H., Yuan Q.H., Synthesis of Nitrogen and Sulfur Co-Doped Yolk-Shell Porous Carbon Microspheres and their Application for Pb(II) Detection in Fish Serum, *J. Solid State Chem.*, **266(10)**: 63-69 (2018).

[31] Wei P., Zhu Z., Song R., Li Z., Chen C., An Ion-Imprinted Sensor Based on Chitosan-Graphene Oxide Composite Polymer Modified Glassy Carbon Electrode for Environmental Sensing Application, *Electrochim. Acta*., **317**: 93-101(2019).

[32] Xie F., Yang M., Jiang M., Huang X. J., Xie P. H., Carbon Based Nanomaterials-A Promising Electrochemical Sensor Toward Persistent Toxic Substance, *Trac-Trends Anal. Chem.*, **119**: 115624-115639 (2019).

[33] Beitollahi H., Safaei M., Tajik S., Different Electrochemical Sensors for Determination of Dopamine as Neurotransmitter in Mixed and Clinical Samples: A Review, *Anal. Bioanal. Chem*., **6(1)**: 81-96 (2019).

[34] Xu H., Zeng L., Xing S., Xian Y., Shi G., Ultrasensitive voltammetric Detection of Trace Lead(II) and Cadmium(II) using MWCNTs-Nafion/Bismuth Composite Electrodes, *Electroanalysis.*, **20(24)**: 2655-2662 (2008).

[35] Beitollahi H., Dourandish Z., Tajik S., Ganjali M. R., Norouzi P., Faridbod F., Application of Graphite Screen Printed Electrode Modified With Dysprosium Tungstate Nanoparticles in Voltammetric Determination of Epinephrine in the Presence of Acetylcholine, *J. Rare. Earth*., **36**: 750-757 (2018).

[36] Hai T.L., Hung L.C., Phuong T., Ha B., Nguyen V.H., Multiwall carbon Nanotube Modified by Antimony Oxide (Sb_2O_3/MWCNTs) Paste Electrode for the Simultaneous Electrochemical Detection of Cadmium and Lead Ions, *Microchem. J*., **153**: 104456-104462 (2019).

[37] Feminus J.J. and Deepa P.N., Electrochemical Sensor Based on Composite of Reduced Graphene and Poly-Glutamic Acid for Selective and Sensitive Detection of Lead, *J. Mater. Sci-Mater El*., **30(16)**: 15553-15562 (2019).

[38] Zhu L., Xu L., Huang B., Jia N., Tan L., Yao S., Simultaneous Determination of Cd(II) and Pb(II) Using Square Wave Anodic Stripping Voltammetry at a Gold Nanoparticle-Graphene-Cysteine Composite Modified Bismuth Film Electrode, *Electrochim. Acta*, **115**: 471-477 (2014).

[39] Wang H., Xu R., Chen H. and Yuan Q., Synthesis of Nitrogen and Sulfur Co-Doped Yolk-Shell Porous Carbon Microspheres and Their Application for Pb(II) Detection in Fish Serum, *J. Solid State Chem.*, **266**: 63-69 (2018).

[40] Hui H., Chen T., Liu X., Ma H., Ultrasensitive and Simultaneous Detection of Heavy Metal Ions Based on Three-Dimensional Graphene-Carbon Nanotubes Hybrid Electrode Materials, *Anal. Chim. Acta*, **852**: 45-54 (2014).

[41] Maleki B., Baghayeri M., Ghanei-Motlagh M., Zonoz F.M., Amiri A., Hajizadeh F., Hosseinifar A., Esmaeilnezhad E., Polyamidoamine Dendrimer Functionalized Iron Oxide Nanoparticles for Simultaneous Electrochemical Detection of Pb^{2+} and Cd^{2+} Ions in Environmental Waters, *Measurement*, **140**: 81-88 (2019).

[42] Zhao Gand Liu G., Synthesis and Characterization of a Single-Walled Carbon Nanotubes/L - Cysteine/Nafion-Ionic Liquid Nanocomposite and Its Application in the Ultrasensitive Determination of Cd(II) and Pb(II), *J. Appl. Electrochem*., **49**: 609-619 (2019).